[8] T. Miteva, A. Meisel, H. Nothofer, U. Scherf, W. Knoll, D. Neher, M. Grell, D. Lupo, A. Yasuda, *Synth. Met.* **2000**, *111–112*, 173.
[9] K. S. Whitehead, M. Grell, D. D. C. Bradley, M. Jandke, P. Strohriegl, *Appl. Phys. Lett.* **2000**, *76*, 2946.
[10] V. N. Bliznyuk, S. A. Carter, J. C. Scott, G. Glärner, R. D. Miller, D. C. Miller, *Macromolecules* **1999**, *32*, 391.
[11] M. Redecker, D. D. C. Bradley, M. Inbasekaran, W. W. Wu, E. P. Woo, *Adv. Mater.* **1999**, *11*, 241.
[12] J. P. Chen, G. Klaerner, J.-I. Lee. D. Markiewicz, V. Y. Lee, R. D. Miller, J. C. Scott, *Synth. Met.* **1999**, *107*, 129.
[13] G. Klaerner, M. H. Davey, W. D. Chen, J. C. Scott, R. D. Miller, *Adv. Mater.* **1998**, *10*, 993.
[14] M. Kreyenschmidt, G. Klärner, T. Fuhrer, J. Ashenhurst, S. Karg, W. D. Chen, V. Y. Lee, J. C. Scott, R. D. Miller, *Macromolecules* **1998**, *31*, 1099.
[15] Y. He, S. Gong, R. Hattori, J. Kanicki, *Appl. Phys. Lett.* **1999**, *74*, 2265.
[16] D. Sainova, T. Miteva, H. G. Nothofer, U. Scherf, H. Fujikawa, I. Glowacki, J. Ulanski, D. Neher, *Appl. Phys. Lett.* **2000**, *76*, 1810.
[17] S. Janietz, D. D. C. Bradley, M. Grell, C. Giebeler, M. Inbasekaran, E. P. Woo, *Appl. Phys. Lett.* **1998**, *73*, 2453.
[18] K. Meerholz, H. Gregorius, K. Müllen, J. Heinze, *Adv. Mater.* **1994**, *6*, 671.
[19] D. M. Pai, J. F. Yanus, M. Stolka, *J. Chem. Phys.* **1984**, *88*, 4414.
[20] C. D. Müller, T. Braig, H. Nothofer, M. Arnoldi, M. Groß, U. Scherf, O. Nuyken, K. Meerholz, *Chem. Phys. Chem.* **2000**, *1*, 207.
[21] M. Jandke, P. Strohriegl, J. Gmeiner, W. Brütting, M. Schwoerer, *Adv. Mater.* **1999**, *11*, 1518.
[22] H. G. Nothofer, *Ph.D. Thesis*, University of Potsdam, Potsdam, Germany **2001**.
[23] T. Yamamoto, *Prog. Polym. Sci.* **1992**, *17*, 1153.
[24] E. P. Woo, M. Inbasekaran, W. Shiang, G. R. Roof, *Int. Patent Appl. WO97/05184*, **1997**.
[25] M. Inbasekaran, W. Wu, E. P. Woo, *US Patent 5 777 070*, **1998**.
[26] A. J. Bard, L. A. Faulkner, *Electrochemical Methods—Fundamentals and Applications*, Wiley, New York **1984**.

Topographical Micropatterning of Poly(dimethylsiloxane) Using Laminar Flows of Liquids in Capillaries**

By *Shuichi Takayama*, *Emanuele Ostuni*, *Xiangping Qian*, *J. Cooper McDonald*, *Xingyu Jiang*, *Phil LeDuc*, *Ming-Hsien Wu*, *Donald E. Ingber*, and *George M. Whitesides**

Structures with micrometer-sized features and patterns will be useful in manipulating cells and studying the effect of microenvironments on cell behavior.[1–3] This paper describes the use of patterned flows of multiple laminar streams of etching solutions in capillaries to create topographical features with sizes of 10–100 μm in poly(dimethylsiloxane) (PDMS); it also demonstrates the use of these topographically patterned capillaries as microchambers for mammalian cell culture. A variety of topographical features can be created by adjusting the widths of the streams, by using channels with obstacles, or by controlling the extent of the etching. Bovine capillary endothelial (BCE) cells show alignment when grown inside these topographically patterned microfluidic channels. The topographical features generated can also be subjected to additional laminar flow patterning of the surface and of the liquid. This two-stage patterning can be used to produce patterns of proteins and cells on the topography, with alignment between the different features and patterns. We believe that these procedures will enable new types of studies in fundamental cell biology, and that they will also be useful in the microfabrication of devices that require a high-level of control over the behavior of cells.

The technique uses multiphase laminar flow—an orderly flow of liquids that occurs at low Reynolds numbers (*Re*), in which different layers of fluids flow side by side without turbulent mixing—to control the pattern of etchant flow.[4–6] The Reynolds number (*Re*) is a non-dimensional parameter describing the tendency of a flowing liquid to develop turbulence (Eq. 1). Here, l is the diameter of the channel [m], v is the flow velocity [m/s], ρ is the density [g/m^3], and η is viscosity [Pa s].[7] Flows with $Re > 2000$ are usually turbulent; flows with low Re (<1) are usually laminar. The flow of liquids in small capillaries often has a low Re, and is laminar, because l is small.[8]

$$Re = lv\rho/\eta \quad (1)$$

The key to the controlled etching of PDMS[9] using laminar flow lies in choosing the appropriate solvent for etching. The solvent must dissolve the product of the etching reaction, but should not significantly swell the cured polymer. Water and ethanol, for example, do not swell PDMS but cannot dissolve etched products. Tetrahydrofuran dissolves etched species but swells PDMS sufficiently that the conformal seal that holds the capillary together breaks. *N*-Methylpyrrolidinone (NMP) dissolves products produced by etchant but swells PDMS only slightly; the slight swelling does not break the conformal seal. All the experiments described in this paper use a solution of tetrabutylammonium fluoride (TBAF) in NMP (3:1; v/v; NMP/75 % TBAF in water) as the etchant. Satisfactory results can also be obtained by substituting dimethylformamide (DMF) or dimethylsulfoxide (DMSO) for NMP.

Experimental Design: Figure 1 describes a typical etching experiment. A network of capillaries is formed by placing a PDMS mold with embedded channel features onto a flat slab of PDMS (glass or silicon wafers can also be used) (Fig. 1A,B). The PDMS mold seals conformally to the PDMS slab and contains the flowing etching solutions within the channels. Fluids are introduced into the capillary system through inlets, and pumped through the channels by aspiration from the outlet at a constant vacuum pressure. Multiple streams of etchant and NMP are allowed to flow side-by-side to give etched and non-etched areas within a capillary. This procedure patterns both the originally flat slab of PDMS and

[*] Prof. G. M. Whitesides, Dr. S. Takayama, E. Ostuni, Dr. X. Qian, J. C. McDonald, X. Jiang, M.-H. Wu
Department of Chemistry and Chemical Biology, Harvard University
12 Oxford Street, Cambridge, MA 02138 (USA)
E-mail: gwhitesides@gmwgroup.harvard.edu
Dr. P. LeDuc, Prof. D. E. Ingber
Departments of Pathology and Surgery
Children's Hospital and Harvard Medical School
Boston, MA 02115 (USA)

[**] We are grateful to the National Institutes of Health (GMW: GM 30367; DEI: PO1 CA45548) and DARPA/ONR for financial support. We also used shared MRSEC facilities supported by NSF under contract number DMR-9809363. ST thanks the Leukemia and Lymphoma Society for a postdoctoral fellowship. EO is grateful to Glaxo Wellcome Inc. for a predoctoral fellowship in organic chemistry. XQ acknowledges the NSERC of Canada for a postdoctoral fellowship.

  0935-9648/01/0804-0570 $ 17.50+.50/0

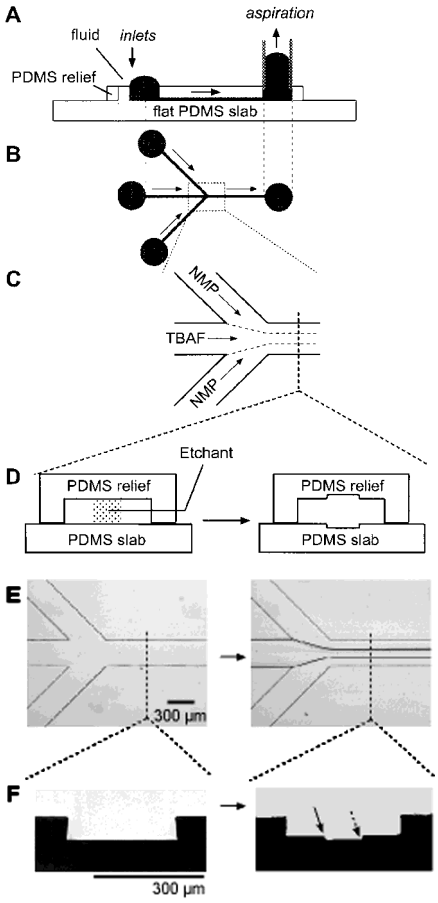

Fig. 1. A typical laminar flow etching experiment. A) Side view perpendicular to the central channel and in the plane of the surface of PDMS. A PDMS relief containing micrometer-sized channels molded in its surface was placed on the surface of a flat PDMS slab to form a network of microfluidic channels. Fluids were pumped by gentle aspiration at the outlet. B) Top view of the channel network. C) A close up view of the junction shows the patterned flow of liquid that is obtained by flowing NMP and TBAF from alternating inlets. D) A schematic representation of a cross-sectional view of the channel before and after etching as seen from the outlet looking towards the inlet. E) Optical micrographs of the PDMS mold before and after etching. F) An optical micrograph of cross sections of the PDMS mold before and after etching. The flat slab of PDMS, which formed the fourth wall of the channel, was removed when taking the image in (E) and (F).

the PDMS mold that has channel features in it (Fig. 1D). The corners produced by the original surface and the etched grooves (Fig. 1F, arrow with solid line) are sharp, but the corners inside the etched grooves (Fig. 1F, arrow with dashed line) are rounded. The slower etching of the corners inside the grooves, compared to the corners at the original surface, probably reflects mass transport. The chemical compositions of the PDMS surfaces before and after etching with the TBAF/NMP solution are indistinguishable by X-ray photoelectron spectroscopy (XPS) (PDMS before etching C: 44 %, O: 31 %, Si: 25 %, F: 0 %; PDMS after etching C: 47 %, O: 29 %, Si: 24 %, F: 0 %). No significant fluorine peak appears in the XPS spectrum of the surface of etchant-treated PDMS. The lack of a fluorine peak in the XPS spectrum of the treated surface suggests that most of the fluoride-containing species dissolve and are carried away. We cannot, however, rule out the possibility of surface rearrangement.[10–12] The fluorine-containing side chains of the polymer may migrate into the bulk polymer so that it is not detected by XPS. The advancing contact angle of PDMS is similar both before and after etching (PDMS before etching 109 ± 5°; PDMS after etching 107 ± 3°). The receding contact angle of PDMS, however, is significantly smaller after the etching procedure (PDMS before etching 98 ± 3°; PDMS after etching 87 ± 4°); we do not know the origin of this difference in the values of the receding contact angles.

Topographical Features That Can Be Created: Figure 2A and B shows how topography of different sizes can be generated by controlling the width of the different fluid streams (the PDMS mold used here was the same as the mold shown in Fig. 1E). The widths of these streams are determined by the relative influx of fluids from each inlet into the main channel. In our setup, the influx of fluids is adjusted by changing the positions of the inlet reservoirs and hence the lengths of the inlet channels; according to the Hagen–Poiseuille law (Eq. 2) for

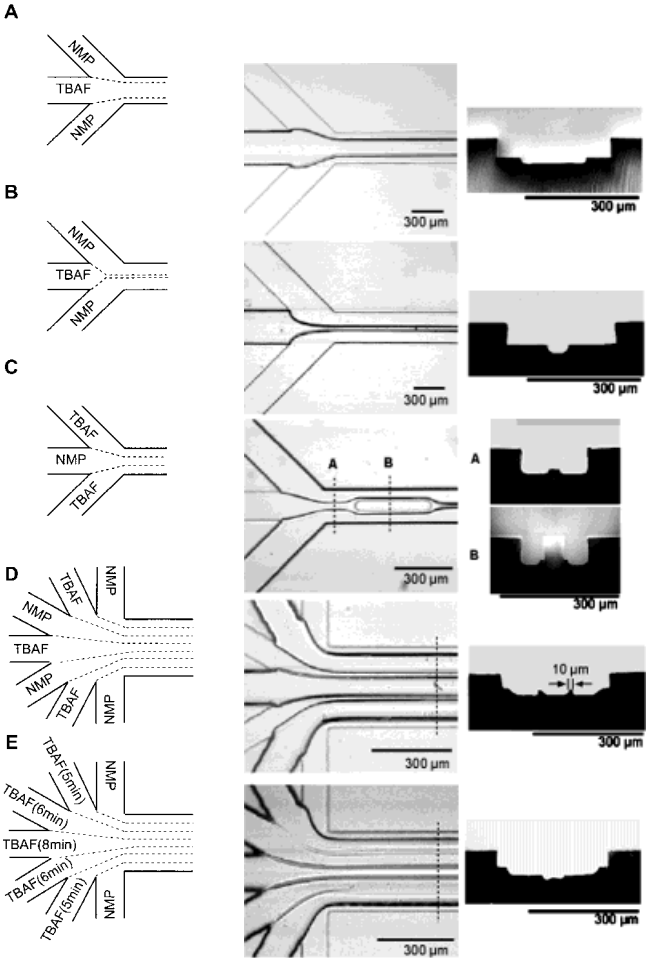

Fig. 2. Examples of features created using laminar flow etching. A) Features of different sizes were created by adjusting the relative volumetric flow rates of the flows from the inlet channels. The etchant (TBAF) and non-etching solution (NMP) were allowed to flow from the designated inlets. In A) and B), the channels were of the same size as the channel in Figure 1; however, the width of the central stream of etchant was wider (A) or narrower (B) than the outer streams of NMP. C) Features created in a channel that had posts fabricated along the center of the main channel. D) Topographical features created in a channel with seven inlets. E) Multiple-level features created by simultaneously controlling both the spatial patterning of the etchant as well as the amount of time the etchant was allowed to flow.

  0935-9648/01/0804-0571 $ 17.50+.50/0

ADVANCED MATERIALS

steady, laminar, fully developed flow in a pipe, volumetric flow rate, Q [m^3/s], is inversely proportional to the length of a channel, given the other parameters are the same.[13]

$$Q \propto \frac{\Delta P R^4}{L\eta} \quad (2)$$

Here, ΔP is the pressure drop across the channel [N/m^2], R is the radius or equivalent radius of the channel [m], L is the length of the channel [m], and η is the viscosity of the medium [$N\ s/m^2$]. Since the initial geometry of all the inlet channels and the pressure drop across the inlet reservoirs and the point at which the inlets converge are all the same, and the viscosity of NMP and TBAF/NMP (1:3) are similar (that is, $\Delta P R^4 \eta^{-1}$ = constant), the relative volumetric flow rates of fluids flowing into the main channel from each inlet are inversely proportional to the length of the inlet channels ($Q \sim L^{-1}$). In the experiment that generated the feature shown in Figure 2A, the length of the middle inlet channel (4 mm) is shorter than that of the outer inlets (9 mm). This results in a higher volumetric flow rate and a wider width of flow in the middle stream. The theoretical ratio of the widths of the different fluid streams calculated from the inlet channel lengths is 1:2.3:1 and the ratio of the widths of the features that were actually obtained is 1:2.4:1. In the procedure resulting in the features shown in Figure 2B, the length of the middle inlet (9 mm) is longer than that of the outer inlets (3 mm). This geometry results in a lower volumetric flow rate and a narrower width of flow for the middle stream. The theoretical ratio of the widths of the different fluid streams calculated from the inlet channel lengths is 3:1:3 and the ratio of the widths of the features that were actually obtained is 2:1:2. Because channel geometry changes as etching proceeds, the widths of the etched features do not match the calculated ratios exactly. The trends, however, are clear and useful for creating topography of different sizes. The differences between the shapes of the etched grooves in Figure 2A through E are a result of the different flow profiles generated during the etching of the grooves; we have not, however, imaged or analyzed these profiles and cannot be certain about their shapes.

Figure 2C shows how obstacles fabricated inside a channel will alter the flow of liquids to create curved features. In this experiment, the PDMS mold has channel features with posts protruding into the channel. In areas of the channel that do not have posts, the flow of etchant creates patterns that are similar to those in the experiment described in Figure 1. In the areas of the channel where there is a post, the flow of liquids has to go around the post; this pattern of flow results in etched features that are curved.

Figure 2D indicates that topographical features can be generated in a seven-inlet capillary. There is no theoretical limit to the number of laminar streams there can be inside of a channel. Channels with large widths should still be able to sustain laminar flows as long as the height of the channel is small.[7] Practical considerations in the size of the channels and the number of inlets that can be fabricated will, however, eventually impose a limit.

An advantage of using laminar flows to create topographical features is the ability to generate multiple-level features in one step. Figure 2E shows staircase-like features that were created by flowing etchant for different durations in different lanes. The amount of time an etchant is allowed to flow over an area determines the amount of etching in that area. A 3:1 NMP/TBAF solution flowing at a rate of 400 μL/min through a rectangular channel (300 × 50 μm) etches PDMS at a rate of 3–5 μm/min. The "exposure time" is adjusted by replacing the TBAF solution in the inlet reservoirs with NMP after the designated amounts of time.

Use of PDMS Capillaries with Topographical Features as Microchambers for Mammalian Cell Culture: Cell shape affects cell growth, gene expression, extracellular matrix metabolism, and differentiation.[1,14] Thus, topographical features that can regulate cell shape have potential applications in the study of fundamental cell biology and in cell-based devices that require the control of cellular behavior.[2,15–18] We tested some of the topographically patterned capillaries as chambers for mammalian cell culture. BCE cells cultured inside capillaries with topographical features elongate along the grooves and ridges of the topography (Fig. 3B,C). Cells cultured inside

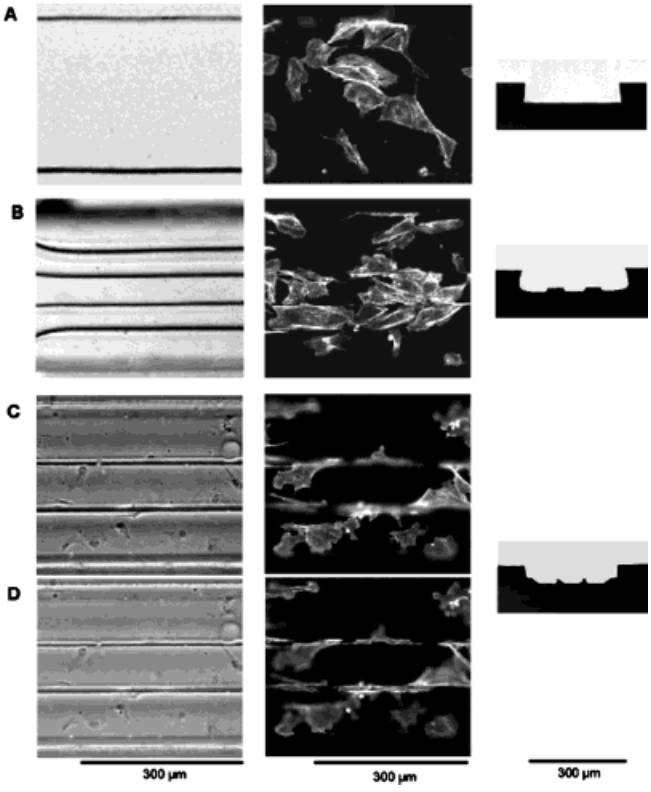

Fig. 3. Alignment of BCE cells on topographical features created by laminar flow etching. A) Control experiment. BCE cells were grown in a channel with no topographical features. Note the random orientation of the cell body as well as the actin stress fibers. B) BCE cells grown in channels with ~60 μm wide ridges and grooves. C) BCE cells grown in channels with ~10 μm ridges and ~80 μm grooves. The left-hand micrograph is a phase-contrast image of the cells after they were fixed and stained with phalloidin to visualize the actin cytoskeleton. The right-hand micrograph is an epi-fluorescence image that shows the actin fibers of the same cells. The cell bodies, as well as the actin stress fibers, align at the edge of the ridges. These micrographs were taken with the focus in the grooves. D) The same BCE cells as in (C) except in these micrographs the focus is in plane with the ridges.

  0935-9648/01/0804-0572 $ 17.50+.50/0

capillaries with flat surfaces spread equally in all directions (Fig. 3A). When we compare cells growing on different parts of the topographical features, we find that BCE cells attached to the ridges show more alignment, compared to cells in the grooves. This enhanced orientation is probably because the ridges have sharper corners compared to the grooves.

Living cells simultaneously detect multiple stimuli such as topography, surface adsorbed proteins, soluble chemicals in the media, and neighboring cells. Laminar flow etching and patterning is a convenient method for patterning multiple stimuli inside a capillary.[3,5] Figure 4A shows a pattern of wheat germ agglutinin labeled with a fluorophore (fluorescein

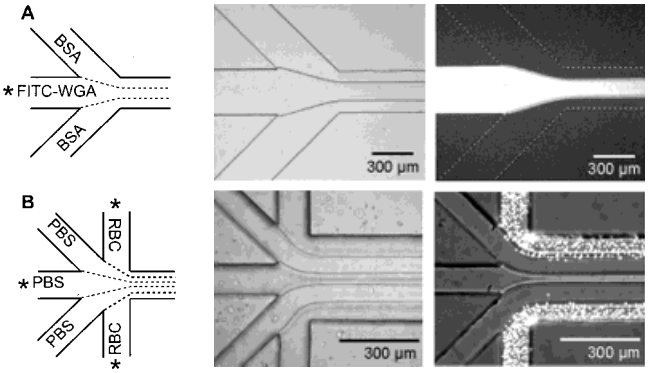

Fig. 4. Patterning adsorption of proteins and attachment of cells in topographically patterned capillaries. The lanes that had been etched are designated by a *. A) Patterned adsorption of protein in a groove created by laminar flow etching of PDMS. Left: Schematic representation of the flow of protein solution. Middle: Optical micrograph of a topographically patterned PDMS channel. Right: Fluorescent micrograph of the pattern of protein (wheat germ agglutinin that was labeled with fluorescein) that adsorbed onto the topographically patterned channel. B) Patterned adsorption of RBCs in grooves created by laminar flow etching. Left: Schematic representation of the flow of RBCs. Middle: Optical micrograph of a topographically patterned PDMS channel. Right: Fluorescence micrograph, with low backlighting, of a pattern of RBCs that adsorbed onto the topographically patterned channel. The RBCs were stained with a fluorescent nucleic acid stain (Syto 9, 15 μM, Molecular Probes).

isothiocanate FITC–WGA) that was generated inside a capillary subsequent to generation of topography. In this experiment, a FITC–WGA solution was allowed to flow from the middle inlet, and a non-fluorescence-labeled protein (bovine serum albumin, BSA) was allowed to flow from the outside inlets. This pattern of flow produces a capillary, in which FITC–WGA adsorption is aligned with the grooved region in the middle portion. Figure 4B shows a pattern of chick red blood cells (RBCs) on topographical features. Here, we allowed a suspension of RBCs to flow from the designated inlets. The alignment of patterns of adsorbed protein and positions of attached cells on the topographical features is straightforward with laminar flow patterning. The only "alignment" necessary is to add the protein solutions or cell suspensions into the appropriate inlet reservoirs and to control the relative flow rates from each inlet.

The ability of multiphase laminar flows to pattern topographical features, protein patterns, and cell positions conveniently with alignment between the different features and patterns provides biology with a broadly useful capability. Although limited in the types of features and patterns that the method can generate, laminar flow etching and patterning has three features that make it complementary to photolithography and to soft lithographic techniques such as microcontact printing, micromolding in capillaries, and replica molding:[19] i) It can control multiple features and patterns without complicated registration steps. Although a number of methods exist for patterning cell stimuli individually in the micrometer scale, their use in generating multiple-component patterns is not straightforward due to the problem of registration of features and patterns. ii) It produces features and patterns inside capillaries and is therefore directly compatible with microfluidic devices, sensors, and labs-on-a-chip. The capillary is sealed conformally. If necessary, the capillary can also be peeled apart to give direct access to the features, patterns, and cells inside. iii) It uses PDMS, a material with several properties that make it attractive for biological applications. It is non-toxic, gas-permeable, and optically transparent. These properties are crucial for culturing cells and for performing optical microscopy.

We believe that laminar flow etching and patterning will enable the fabrication of systems useful in studying, simultaneously, the effect of multiple extracellular stimuli—such as, topographical feature of the substrate, molecular structure of the substrate, the nature and position of neighboring cells, and the composition of the surrounding fluid—on cell behavior; these methods will also be useful in the development of microfluidic systems for cell-based assays and cell-based sensors.

Experimental

Device Fabrication: PDMS molds were formed by curing prepolymer (Sylgard 184, Dow Corning) on a silanized Si master having a positive relief (~55 μm) of the capillary channels formed in photoresist (SU-8-50, MicroChem Corp.) on its surface [11]. Inlet and outlet reservoirs were defined by creating holes in the PDMS mold using a pipe with sharpened edges (5 mm diameter). PDMS molds with embedded channel features and reservoirs were placed on flat slabs of PDMS resulting in formation of the capillary channels. The PDMS pieces sealed against each other conformally.

Creating Topography: Initially, all reservoirs and channels were filled with a non-etching solvent (NMP). Solvent in select inlet reservoirs was replaced with etchant (3:1; v/v; NMP/75 % TBAF in water). Fluids were pumped by aspiration from the outlet at initial volumetric flow rates of ~50–200 μL/min. The volumetric flow rates increased as the etching proceeded and the cross-sectional area of the channel increased. This range of flow rates was optimal for obtaining sharp features; the flow needed to be fast enough to minimize lateral diffusion of etchant molecules but not so extremely fast that the formation of eddies and chaotic advection became significant. After etching for the desired amount of time (3 min unless noted otherwise) the etchant was diluted with non-etching solvent. NMP was pumped through the system for an additional 10 min to ensure removal of all etchant. Micrographs of the features were taken after peeling apart the PDMS pieces. To obtain cross-sectional micrographs, etched PDMS molds were cut in a direction perpendicular to the length of the channel with a scalpel, and the newly exposed surface was viewed with a microscope.

Patterning Proteins and Cells: We used PDMS replicas of etched features to ensure that the patterning of proteins and cells was not influenced by differences in the surface chemistry produced by the etching procedure. Molds of the topographical features were prepared by curing an epoxy resin (Epo-tek, Epoxy Technology, Billerica, MA) against the original etched features. PDMS replicas were obtained by curing prepolymer against this epoxy mold. The replicas were sealed against a flat slab of PDMS to produce channels with topographical features.

  0935-9648/01/0804-0573 $ 17.50+.50/0

ADVANCED MATERIALS

Bovine adrenal capillary endothelial (BCE) cells were cultured and harvested as previously reported [20]. In brief, cells were cultured under 10 % CO_2 on Petri dishes (Falcon) coated with gelatin in Dulbecco's modified eagle's medium (DMEM, Gibco) containing 10 % calf serum, 2 mM glutamine, 100 μg/mL streptomycin, 100 μg/mL penicillin, 1 ng/mL basic fibroblast growth factor (bFGF). Cells were dissociated from culture plates with trypsin/ethylenediamine tetraacetate (EDTA) and washed in DMEM containing 1 % w/v BSA (BSA/DMEM). These cells were suspended in medium (10 % calf serum/DMEM) [20], and introduced into capillary networks (pretreated with 50 μg/mL fibronectin for 1 h) from the reservoirs and incubated in 10 % CO_2 at 37 °C for 6 h. Cells were fixed with paraformaldehyde (4 % in phosphate buffered saline, PBS, Electron Microscopy Sciences), treated with detergent (0.5 % triton X-100 in PBS, Sigma) for 2 min, and stained for actin (phalloidin-Alexa 594, Molecular Probes, for 2 h). The PDMS pieces were peeled apart and the sample mounted with Fluoromount G (Electron Microscopy Sciences) and a glass coverslip. Micrographs were taken through the glass coverslip (Fig. 3).

Protein solutions (1 mg/mL FITC–WGA in PBS, Sigma; 10 mg/mL BSA in PBS, Sigma) were pumped at volumetric flow rates of ~50–200 μL/min by aspiration from the outlet. RBC suspensions (12 day old chick erythrocytes, 5 mL cells in 165 mL Alsever's solution, SPAFAS, Preston, CT) were pumped at volumetric flow rates of ~5 μL/min by hydrostatic pressures created by differences in fluid levels between the inlet and outlet reservoirs. After patterning for the desired amounts of time (10 min for proteins and 5 min for erythrocytes) the channels were washed with PBS for 10 min. Micrographs of the protein and erythrocyte patterns were obtained through PDMS, with PBS present in the channel, and without peeling apart the PDMS pieces that make up the channel (Fig. 4).

Received: September 22, 2000
Final version: December 14, 2000

[1] C. S. Chen, M. Mrksich, S. Huang, G. M. Whitesides, D. E. Ingber, *Science* **1997**, *276*, 1425.
[2] R. G. Flemming, C. J. Murphy, G. A. Abrams, S. L. Goodman, P. F. Nealey, *Biomaterials* **1999**, *20*, 573.
[3] S. Takayama, R. G. Chapman, R. S. Kane, G. M. Whitesides, in *Principles of Tissue Engineering*, 2nd ed. (Eds: R. P. Lanza, R. Langer, J. Vacanti), Academic, San Diego, CA **2000**, p. 209.
[4] B. H. Wiegl, P. Yager, *Science* **1999**, *283*, 346.
[5] S. Takayama, J. C. McDonald, E. Ostuni, M. N. Liang, J. A. Kenis, R. F. Ismagilov, G. M. Whitesides, *Proc. Natl. Acad. Sci. USA* **1999**, *96*, 5545.
[6] P. J. A. Kenis, R. F. Ismagilov, G. M. Whitesides, *Science* **1999**, *285*, 83.
[7] P. W. Atkins, *Physical Chemistry*, Freeman, New York **1994**.
[8] G. T. A. Kovacs, *Micromachined Transducers Sourcebook*, WCB/McGraw-Hill, New York **1998**.
[9] B. Xu, F. Arias, G. M. Whitesides, *Adv. Mater.* **1999**, *11*, 492.
[10] S. Clark, M. C. Davies, C. J. Roberts, S. J. B. Tendler, P. M. Williams, *Langmuir* **2000**, *16*, 5116.
[11] D. C. Duffy, J. C. McDonald, O. J. A. Schueller, G. M. Whitesides, *Anal. Chem.* **1998**, *70*, 4974.
[12] M. Morra, E. Occhiello, R. Marola, F. Garbassi, P. Humphrey, D. Johnson, *J. Colloid Interface Sci.* **1990**, *137*, 11.
[13] I. Granet, *Fluid Mechanics for Engineering Technology*, 3rd ed., Prentice Hall, Englewood Cliffs, NJ **1989**.
[14] S. Huang, D. E. Ingber, *Nature Cell Biol.* **1999**, *1*, E131.
[15] H. C. Hoch, R. C. Staples, B. Whitehead, J. Comeau, E. D. Wolf, *Science* **1987**, *235*, 1659.
[16] M. Mrksich, C. S. Chen, Y. Xia, L. E. Dike, D. E. Ingber, G. M. Whitesides, *Proc. Natl. Acad. Sci. USA* **1996**, *93*, 10775.
[17] A. Curtis, C. Wilkinson, *Biomaterials* **1997**, *18*, 1573.
[18] E. T. den Braber, J. E. de Ruijter, L. A. Ginsel, A. F. von Recum, J. A. Jansen, *J. Biomed. Mater. Res.* **1998**, *40*, 291.
[19] Y. Xia, G. M. Whitesides, *Angew. Chem. Int. Ed.* **1998**, *37*, 550.
[20] D. E. Ingber, J. Folkman, *Proc. Natl. Acad. Sci. USA* **1990**, *87*, 3579.

Hybrid Langmuir–Blodgett Films Formed by Alternating Layers of Magnetic Polyoxometalate Clusters and Organic Donor Molecules—Towards the Preparation of Multifunctional Molecular Materials**

By *Miguel Clemente-León*, *Eugenio Coronado*,* *Pierre Delhaes*, *Carlos J. Gómez-García*, and *Christophe Mingotaud**

Polyoxometalates (POMs) constitute a wide class of inorganic compounds with remarkable chemical, structural, and electronic versatility that have applications in areas such as catalysis, medicine, and materials science.[1] In view of the ability of these molecular metal-oxide clusters to act as electron acceptors and to accommodate magnetic transition metal centers in their structures, they have been used as inorganic components in the construction of hybrid organic–inorganic functional materials. For example, in crystalline solids based on tetrathiafulvalene (TTF)-type organic donors, the magnetic moments localized in the POM clusters coexist with the conducting electrons of the organic network.[2] Other organic–inorganic hybrids are those in which POMs are embedded in conductive polymer films, such as polypyrrole, polyaniline, or polythiophene.[3] A third class of hybrids are the Langmuir–Blodgett (LB) films based on POMs.[4] Recently, we have shown that these polyanions can be organized as monolayers when they are in the presence of a positively charged monolayer of an organic surfactant, such as the dimethyldioctadecylammonium (DODA) cation spread on water. In these organized lamellar structures, the monolayers of POMs alternate with bilayers of DODA to afford centrosymmetrical LB films. This is a general method and has been used to insert a variety of POMs of increasing nuclearities between the organic layers.[5] Thus, monolayers of magnetic POMs of the type $[Co_4(H_2O)_2(PW_9O_{34})_2]^{10-}$ and $[Co_4(H_2O)_2(P_2W_{15}O_{56})_2]^{16-}$ that encapsulate a Co_4O_{16} ferromagnetic cluster,[6] and the giant POM $[Co_9(OH)_3(H_2O)_6(HPO_4)_2(PW_9O_{34})_3]^{16-}$ and $[Ni_9(OH)_3(H_2O)_6(HPO_4)_2(PW_9O_{34})_3]^{16-}$ based on a nonanuclear M_9O_{36} magnetic cluster have been constructed. More recently, Volkmer and co-workers have combined DODA molecules with the high nuclearity heteropolyoxomolybdates $[H_3Mo_{57}V_6(NO)_6O_{183}(H_2O)_{18}]^{21-}$ and $[Mo_{132}O_{372}(CH_3COO)_{30}(H_2O)_{72}]^{42-}$, obtained from Müller's group, to

[*] Prof. E. Coronado, Dr. M. Clemente-León, Dr. C. J. Gómez-García
Instituto de Ciencia Molecular, Univ. de Valencia
Dr. Moliner 50, E-46100 Burjasot (Spain)
E-mail: eugenio.coronado@uv.es
Dr. C. Mingotaud, Dr. P. Delhaes
Centre de Recherche Paul Pascal, CNRS
Avenue A. Schweitzer, F-33600 Pessac (France)
E-mail: mingotaud@crpp.u-bordeaux.fr

[**] This work has been performed in the framework of the European COST Action 518 (Project on Magnetic Properties of Molecular and Polymeric Materials). Financial support from the Spanish Ministerio de Ciencia y Tecnología (Grants MAT98-0880 and 1FD97-1765) is gratefully acknowledged. The authors are indebted to J. Amiel for EPR measurements.

  0935-9648/01/0804-0574 $ 17.50+.50/0